Discrete Material and Thickness Optimization of laminated composite structures including failure criteria

Lund, Erik

Published in:
Structural and Multidisciplinary Optimization

DOI (link to publication from Publisher):
10.1007/s00158-017-1866-2

Publication date:
2018

Document Version
Early version, also known as pre-print

Discrete Material and Thickness Optimization of laminated composite structures including failure criteria

Erik Lund*

Department of Materials and Production,
Aalborg University,
Fibigerstraede 16, 9220 Aalborg East, Denmark

Published in Structural and Multidisciplinary Optimization,
December 2017, http://dx.doi.org/10.1007/s00158-017-1866-2

Abstract

This work extends the Discrete Material and Thickness Optimization approach to structural optimization problems where strength considerations in the form of failure criteria are taken into account for laminated composite structures. It takes offset in the density approaches applied for stress constrained topology optimization of single-material problems and develops formulations for multi-material topology optimization problems applied for laminated composite structures. The method can be applied for both stress- and strain-based failure criteria. The large number of local constraints is reduced by the use of aggregate functions, and the developed approach is demonstrated for optimization problems involving both constant and varying thickness laminated composites.

Keywords Discrete Material Optimization; Discrete Material and Thickness Optimization; Failure criteria; Laminated composites

1 Introduction

Laminated composite structures consisting of Glass or Carbon Fiber Reinforced Polymers (GFRP/CFRP) make it possible to achieve efficient and lightweight structural designs due to their superior strength and stiffness characteristics. The large design freedom associated with these structures makes it attractive to apply structural optimization techniques in the design process, and many different approaches have been developed since the earliest works like Schmit and Farshi (1973) in the seventies. An overview of optimization methods for laminated composites can be found in Ghiasi et al. (2009) and Ghiasi et al. (2010), where the methods are divided into constant and variable stiffness methods. One of the methods for variable stiffness design is the family of Discrete Material Optimization (DMO) approaches by Stegmann and Lund (2005) and Lund and Stegmann (2005), and these parameterization approaches are applied in this paper.

Laminated composites are built of layers of e.g. GFRP or CFRP, and in case of sandwich structures a light-weight core material like PVC foam or balsa wood are placed inside the structure. Thus, the designer can decide on the type of material and layer (ply) thickness and in case of fiber reinforced materials also the fiber orientation. In many cases the material has to be oriented at given chosen angles, e.g., $-45°$, $0°$, $45°$, and $90°$ due to design guidelines. Thus, the design problem from the starting point is a combinatorial problem that require integer or combinatorial optimization. However, as it is much easier to solve continuous optimization problems using gradient based optimization, much work has been done using continuous thicknesses and fiber orientations as design variables.

Due to the stiffness properties of the orthotropic materials applied for laminated composites, the optimization problems often have multiple solutions with the same performance. For example, fiber orientations of $-45°$ and $45°$ for a unidirectional (UD) GFRP may be equally good in many design problems. Gradient based optimization using thicknesses and fiber orientations directly as design variables may easily end in a local minima due to a nonconvex design space, and the material choice problem of selecting, e.g., GFRP, CFRP or foam material cannot be handled by this parameterization. It is important to note that thickness optimization of plates and shells is an ill-posed optimization problem that needs some kind of regularization as described for solid isotropic elastic plates in Cheng and Olhoff (1981, 1982). For laminated composites this is typically achieved by adding constraints on the allowable rate of thickness variation, i.e. ply-drop constraints, or by using a patch parameterization where a number of finite elements in the numerical model are enforced to have the same thickness.

A very popular method for optimization of laminated composites is genetic algorithms (GA). Very often the layer thickness of each material is fixed, and the fiber orientations are limited to a set of discrete values. Then the optimization problem is reduced to a discrete stacking sequence problem, and Haftka, Gürdal and their coworkers in the 1990s developed specialized GAs for stacking sequence optimization, see e.g. Le Riche and Haftka (1993, 1995), Gürdal et al. (1994), Kogiso et al. (1994), and Nagendra et al. (1996). The advantage of GAs and

* Email: el@mp.aau.dk

many other meta-heuristic algorithms is that they return a number of near optimal designs with only minor variation in performance index instead of a single design. Many other global optimization algorithms dedicated to optimization of laminated composites have also been developed. Stacking sequence optimization of laminated composite structures to satisfy requirements on ply continuity (also referred to as blending) has been studied by many including Gürdal et al. (1999), Kristinsdottir et al. (2001), Liu and Haftka (2001), Seresta et al. (2007), Liu et al. (2011), Zein et al. (2012), Liu et al. (2015), and Zein et al. (2016). Recent work on stacking sequence optimization including blending and ply-drop design guidelines include Irisarri et al. (2014, 2016) and Peeters and Abdalla (2016).

For monolithic laminates a very popular parameterization approach is to apply lamination parameters as introduced by Tsai and Pagano (1968). The laminate stiffnesses are linear functions of lamination parameters, which has convexity advantages for stiffness design problems. Furthermore, the number of design variables is independent of the number of layers, so the number of design variables can be reduced significantly for laminates with many layers. The relationships between in-plane and out-of-plane lamination parameters are available for a number of cases, such that gradient based optimization can be performed efficiently using lamination parameters, see e.g. Miki and Sugiyama (1993), Hammer et al. (1997), Gürdal et al. (1999), Herencia et al. (2008), and Bloomfield et al. (2009).

Liu et al. (2000) presented a two-step (global and bottom) strategy for minimizing the mass of composite wing panels subject to strain and buckling constraints, and similar bi-level approaches have been applied by many including Herencia et al. (2008), IJsselmuiden et al. (2009) and Liu et al. (2011). In the first step the laminate is parameterized using lamination parameters, and a number of industry layup rules can be imposed on the feasible region for the lamination parameters, for example by restricting the design space to symmetric and balanced laminates. Nonsymmetric laminates may warp in response to an applied uniform temperature change across their thickness. This warping can occur during cool-down from the cure temperature during manufacturing and during in-service operations, and thus many design guidelines require symmetric layups. The optimization problem at the global level (first step) was solved efficiently using gradient based optimization, and a GA was used at the bottom level (second step) to optimize the stacking sequence in order to meet the target values of lamination parameters coming from the top level. A number of different approaches have been developed for the bottom level problem in order to obtain realizable laminate designs that satisfy structural constraints as well as manufacturing constraints governed by layup rules. The two-step approach may have some drawbacks as pointed out by Zein and Bruyneel (2015) because the stacking sequences determined at the bottom level do not have a direct control over the thicknesses determined at the global level. They proposed a new algorithm such that the optimization problem is solved without splitting it into two steps as in common practice.

The approach applied by Altair Engineering in the commercial software OptiStruct relies on a three-phase optimization process guiding the composite laminate designs from a concept to the final ply-book details, see Zhou et al. (2011) and Zhou and Fleury (2012). The first phase concerns the conceptual ply layout, the second phase determines the specific number of plies, and the last phase determines the final stacking sequence of the laminate, taking performance demands and manufacturing constraints into account.

Typically strength requirements are taken into account in the form of strain constraints when applying lamination parameters, due to lack of information about the actual laminate configuration, and the failure envelope is dependent on ply angles and thicknesses. To overcome this problem IJsselmuiden et al. (2008) proposed to find the region in strain space that is safe regardless of the ply angles, such that a conservative Tsai-Wu failure envelope in the laminate parameter space was obtained. Unlike minimum compliance problems, there is no analytical proof that strength optimization with lamination parameters is convex and thus global optimality is not assured. Khani et al. (2011) proposed a convexifying approach, where a hybrid approximation for the failure index was developed.

The definition of lamination parameters is valid for monolithic laminates, and thus the optimization procedures described above can only be applied for such single-material laminates. However, de Faria (2015) extended the definition of laminate parameters to allow for hybrid laminates, and thus it should be possible to apply this parameterization for multi-material laminates.

In this work the aim is to be able to optimize multi-material laminated composites while taking failure criteria into account, and the Discrete Material Optimization (DMO) parameterization approaches are applied, as they can be applied for any combination of materials. In the DMO method a number of candidate materials are defined, which could be different FRP materials oriented at given chosen angles, e.g., $-45°$, $0°$, $45°$, and $90°$. The discrete problem of choosing the best candidate material is converted to a continuous problem that can be solved efficiently using gradient based optimizers. Multi-material interpolation functions with penalization of intermediate design variable values are applied, and the first DMO interpolation functions as described in detail in Stegmann and Lund (2005) were self-balancing with the aim of obtaining a distinct choice of material. As an alternative to the self-balancing procedure, Hvejsel et al. (2011) introduced a series of linear equality constraints to ensure that the sum of weighting functions for the candidate materials would equal unity. Here the distinct selection of a single candidate was achieved by a non-linear inequality constraint. Hvejsel and Lund (2011) introduced an alternative to the explicit non-linear constraint by proposing multi-material variations of the well-known SIMP and RAMP interpolation schemes, see Bendsøe (1989) and Stolpe and Svanberg (2001), respectively. Blasques and Stolpe (2012) also applied such interpolation schemes for multi-material topology optimization of laminated composite beam cross sections, and this parameterization approach has been the preferred choice in our work for constant thickness laminates since 2011. With these multi-material variations of the SIMP and RAMP interpolation schemes, linear

equality constraints are introduced to ensure that the sum of design variables for the candidate materials is equal to unity. Nonlinear interpolation functions are applied by appropriate choice of penalization parameter in the SIMP and RAMP interpolation schemes in order to make intermediate design variable values unfavourable. As an alternative, Kennedy and Martins (2013) used linear interpolation and added a series of non-linear equality constraints as a penalty term to the objective function, effectively penalizing intermediate design variable values.

An alternative to these DMO interpolation functions is the Shape Functions with Penalization (SFP) method proposed by Bruyneel (2011) where the author applied four node shape functions known from the finite element method to interpolate between four material candidates using only two design variables. The SFP method was later extended to include three and eight node elements, see Bruyneel et al. (2011). The SFP method was generalized by Gao et al. (2012) by introducing the Bi-valued Coding Parameterization (BCP) method which has no upper limit on the number of applied material candidates. The main advantage of SFP and BCP methods is the substantial reduction of the number of design variables required to do the material interpolation compared to the other DMO interpolation schemes. Furthermore, no linear equality constraints are needed. However, the results of the BCP method may depend on the numbering of the candidate materials, if the number of design variables is different from 2,4,8,16, etc. Kiyono et al. (2017) has recently proposed a new parameterization approach named Normal Distribution Fiber Optimization (NDFO) for fiber angle optimization. It takes offset in the same formulation as DMO, SFP and BCP, but only one design variable is needed to any number of candidates. The normal distribution function is used as a parameterization of the weighting functions, and the formulation is straightforward to implement. A filtering technique can be easily implemented to achieve fiber continuity, and good convergence properties have been reported.

As mentioned previously, for laminated composite structures thickness variations are often needed in order to optimize the design. The thickness variations are accomplished by dropping plies along the length to match varying in-plane and bending loads. Sørensen and Lund (2013) proposed an extension to the DMO method for simultaneously determining an optimum thickness variation and material distribution. The proposed method was developed for problems concerning mass constrained minimization of compliance. Sørensen et al. (2014) extended the work and proposed the Discrete Material and Thickness Optimization (DMTO) method. In the DMTO approach the DMO multi-material interpolation schemes are extended by including a topology (density) variable so to effectively terminate individual plies throughout the laminate. The DMTO method was demonstrated on a generic main spar used in some designs of wind turbine blades where the objective was to minimize the total mass while maintaining structural performance by means of constraints on buckling load factors, eigenfrequencies, and displacements.

The DMO and DMTO approaches are typically implemented in in-house finite element codes with full access to the source code, but it has recently been demonstrated in Wu et al. (2017) how the DMO approach can be implemented in a commercial finite element code for compliance problems including eigenfrequency and local displacement constraints. However, the DMO and DMTO approaches have only been applied for structural criteria like compliance, eigenfrequencies, buckling load factors, and displacements. In this work it will be described how the approaches can be extended to take strength criteria into consideration in the optimization formulation.

The inclusion of strength criteria in structural topology optimization problems is a challenging problem due to the local nature of these criteria and their behaviour in the context of topology optimization. Sved and Ginos (1968) described how stress constraints can be violated for truss topology optimization problems when the bar area goes to zero, such that it can not be removed, and they discovered singular optimal topologies. The singularity problem is discussed in many papers, see e.g. Kirsch (1990), Cheng and Jiang (1992), Rozvany and Birker (1994) and Guo et al. (2001). The singularity problem may also appear in laminate design where these singular optima are linked to the removal of zero thickness plies from the stacking sequence as demonstrated in Bruyneel and Duysinx (2006). One way to avoid the singularity problem is to use an ϵ-approach as suggested by Cheng and Guo (1997) for truss topology optimization. This ϵ-approach was adopted by Duysinx and Sigmund (1998) and Duysinx and Bendsøe (1998) for stress constrained topology optimization of continuum structures. Due to the local nature of stress constraints, such topology optimization problems are computationally challenging due to the high number of design variables and local constraints. In order to reduce the computational effort Duysinx and Sigmund (1998) introduced a global stress measure using two different P-norm methods, such that all stresses were grouped into a single stress constraint. This reduced the computational effort by orders of magnitude because the size of the mathematical programming problem became much smaller and the design sensitivity analysis was much faster due to the use of an adjoint formulation. However, using only a single global stress measure made it difficult to control the local stress level. This was also observed in the work by Yang and Chen (1996) where two different global stress measures were investigated.

The ϵ-approach consists of solving a sequence of problems for decreasing values of the ϵ relaxation parameter, and its successful application has been demonstrated for many different types of topology optimization problems. An ϵ-approach that regularizes the stress singularity for vanishing material selection and topology variables using the DMTO parameterization and solved using a barrier method tailored for stress-constrained mass minimization has been developed in Kennedy (2016). In recent years the most popular approach for stress constrained topology optimization has been to use a SIMP type relaxation as introduced in Bruggi (2008). In this approach a SIMP interpolation scheme is used for stress constraints, using suitable penalization exponents that are different from those that interpolate stiffness parameters.

The success of stress constrained topology optimization

relies on the application of clustering the large number of local stress constraints into a lower number of global stress constraints. Reviews of existing results obtained using local and global stress constraints can be found in Le et al. (2010). It is difficult to find a general and robust function for clustering the local stress constraints, such that the local peak values are controlled efficiently. The most commonly used functions are *P*-norm functions (Duysinx and Sigmund, 1998; Holmberg et al., 2013; Le et al., 2010) and Kreisselmeier-Steinhauser (KS) functions (Kennedy and Martins, 2014; Kreisselmeier and Steinhauser, 1979; París et al., 2009; Yang and Chen, 1996). In many recent works the local and global stress constraint approaches are combined as in the regional stress measure approach by Le et al. (2010) and the block aggregation approach by París et al. (2010). This makes it possible to reduce the large number of constraints efficiently by using global stress measures, but the number of local stresses included in each aggregate function is limited in order to improve the accuracy of the constraint lumping.

This work can be considered as an extension of stress constrained topology optimization using density approaches to multi-material topology optimization problems where the parameterizations applied are the DMO and DMTO approaches for laminated composites. As in the work of Bruggi (2008) and subsequent topology optimization papers with stress constraints, suitable penalization parameters are introduced in the parameterizations. Combined with the use of aggregate functions for reducing the large number of local strength values, it will be shown how challenging optimization problems related to design of laminated composite structures can be solved.

The analysis will be based on layered shell finite elements using Reissner-Mindlin assumptions, i.e. first order shear deformation theory. These finite elements are commonly used for stress analysis of laminated composite structures, as they give a good estimation of the overall strain and stress distributions through-the-thickness of the laminate. However, local effects and out-of-plane stresses will not be captured accurately, and thus it is advantageous to include design rules/manufacturing constraints that implicitly limit these effects. Two manufacturing constraints described in detail in Sørensen and Lund (2013) for the DMTO parameterization will be applied. The first is a constraint on the allowable rate of thickness variation, i.e. a ply-drop constraint, so to avoid abrupt changes in stiffness which can lead to delamination. The second is a so-called contiguity constraint that defines an upper limit on the number of identical contiguous plies, as larger transverse stresses may be build-up in thick plies, again leading to a larger risk of delamination failure.

The remaining of the paper is organized as follows. First, the DMO and DMTO parameterizations are presented in Section 2. This is followed by a description of the failure analysis developed for computing effective failure indices for the multi-material topology problem in Section 3. The gradient based optimization approach is described in Section 4 before four different numerical examples are presented and discussed in Section 5. Finally, Section 6 contains the overall conclusions of the work.

2 Parameterization

In the following the parameterizations applied for constant and varying thickness laminates are described.

2.1 Design parameterization using DMO

In case of optimizing constant thickness laminates, the design parameterization is based on the DMO formulation by Stegmann and Lund (2005), Lund and Stegmann (2005) and Hvejsel and Lund (2011). The laminated composite structure is modeled by layered shell finite elements, and the structure is divided into a number of patches, consisting of a number of finite elements, where the same layup should apply. A number of candidate materials, n^c, are defined for each material patch p. The candidate materials can be, for example, a unidirectional (UD) fiber reinforced polymer (FRP) material oriented at different chosen fiber angles together with possible core materials in case of designing sandwich structures as illustrated in Figure 1. The number of layers of the laminate is denoted n^l.

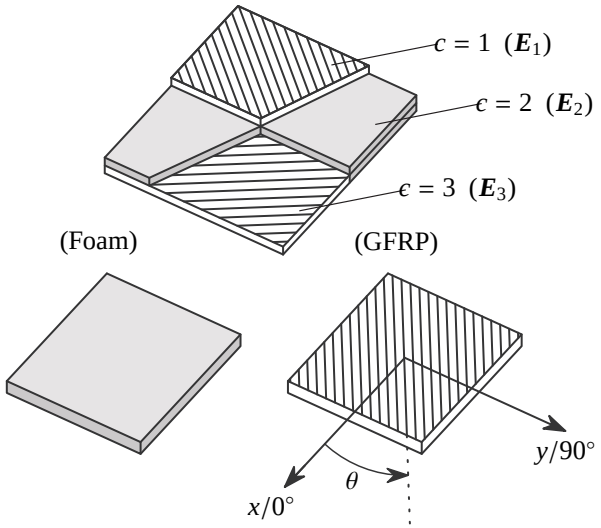

Figure 1: *Top:* Potential outcome of a tapered laminated plate example. *Bottom:* Each material candidate c is described by the constitutive matrix $\boldsymbol{E}_c$. Material candidates can be, for example, a foam type (left) or glass fiber reinforced polymer (GFRP) fiber mats (right), characterized by the fiber orientation θ.

The candidate material variables x_{plc} are defined for all n^p material patches such that

$$x_{plc} = \begin{cases} 1 & \text{if candidate } c \text{ is selected in layer } l \text{ of patch } p \\ 0 & \text{otherwise} \end{cases} \tag{1}$$

The constitutive matrix $\boldsymbol{E}_{el}$ for a given layer l in a given shell element e contained in patch p is thus determined by

$$\boldsymbol{E}_{el} = \sum_{c=1}^{n^c} x_{plc} \boldsymbol{E}_c \tag{2a}$$

$$\sum_{c=1}^{n^c} x_{plc} = 1 \qquad \forall (p,l) \tag{2b}$$

$$x_{plc} \in \{0;1\} \qquad \forall(p,l,c) \qquad (2c)$$

where $\boldsymbol{E}_c$ is the constitutive matrix associated with material candidate c and (2b) is a resource constraint which ensures that only one distinct material candidate can be selected.

The combinatorial problem of selecting the material candidate variables x_{plc} is converted to a continuous problem using interpolation functions with penalization, such that it is possible to apply efficient gradient based optimization algorithms for solving the multi-material topology optimization problem. The multi-material generalizations of the well-known SIMP and RAMP interpolation schemes, see Bendsøe (1989) and Stolpe and Svanberg (2001), respectively, can be used as proposed in Hvejsel and Lund (2011), see also Blasques and Stolpe (2012). Thus, the integer problem is relaxed by treating the design variables x_{plc} as continuous variables, i.e. the method can be considered as a multi-material density approach. The constitutive properties for a given layer l in a given element e associated with patch p are now interpolated as

$$\boldsymbol{E}_{el} = \sum_{c=1}^{n^c} w(\boldsymbol{x})\, \boldsymbol{E}_c \qquad (3a)$$

$$\sum_{c=1}^{n^c} x_{plc} = 1 \qquad \forall(p,l) \qquad (3b)$$

$$x_{plc} \in [0;1] \qquad \forall(p,l,c) \qquad (3c)$$

The weight function $w(\boldsymbol{x})$ for the multi-material generalized SIMP scheme is given as

$$w(\boldsymbol{x}) = x_{plc}^{q} \qquad (4)$$

whereas for the generalized RAMP scheme it is given as

$$w(\boldsymbol{x}) = \frac{x_{plc}}{1 + q(1 - x_{plc})} \qquad (5)$$

Here q is a penalization factor and $\boldsymbol{E}_c$ the constitutive matrix for candidate c in the given layer. Penalization of intermediate design variable values x_{plc} is necessary as the optimizer otherwise can generate superior, but non-physical, pseudo materials by combining the properties of different material candidates. With these interpolation schemes the design variables x_{plc} can be considered as volume fractions of each material candidate as seen from the resource constraint (3b). If holes are allowed in the structure, then the resource constraint (3b) should be changed to a less-than constraint, see examples in Hvejsel and Lund (2011).

This generalized RAMP parameterization for multi-material topology optimization leads to very many sparse linear constraints due to the resource constraint (3b), and thus it is necessary to apply an optimization algorithm that can handle such linear constraints efficiently. Design sensitivity analysis of criterion function will involve derivatives of the constitutive properties, which are found analytically by differentiation of (3a).

2.2 Design parameterization using DMTO

The DMO approach was extended to varying thickness laminates in Sørensen and Lund (2013) and Sørensen et al. (2014) where the Discrete Material and Thickness Optimization (DMTO) approach was developed, making it possible to simultaneously determine an optimum thickness variation and material distribution of the laminated composite structure. The idea is to introduce a density variable to govern the presence of material in a given layer, and thereby determine the thickness variation throughout the laminate. The layerwise density variables can be defined either on element level or by groups of elements having the same thickness. In this work, they are defined by groups of elements termed geometry design domains as illustrated in Figure 2 such that

$$\rho_{dl} = \begin{cases} 1 & \text{if there is material in layer } l \text{ for domain } d \\ 0 & \text{otherwise} \end{cases} \qquad (6)$$

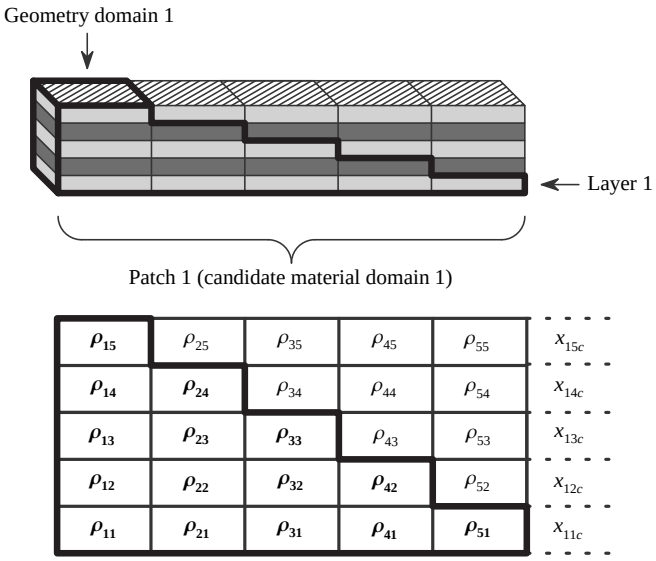

Figure 2: Example of a patch (candidate material domain 1) combined with 5 geometry domains. The design variables associated with the domains are listed.

In a similar way as described for the material design variables, the density variables ρ_{dl} are treated as continuous variables and the constitutive properties for a given layer l in a given element e associated with material patch p and geometry domain d are now interpolated as

$$\boldsymbol{E}_{el} = \sum_{c=1}^{n^c} w(\boldsymbol{x},\boldsymbol{\rho})\, \boldsymbol{E}_c \qquad (7a)$$

$$\sum_{c=1}^{n^c} x_{plc} = 1 \qquad \forall(p,l) \qquad (7b)$$

$$x_{plc} \in [0;1] \qquad \forall(p,l,c) \qquad (7c)$$

$$\rho_{dl} \in [0;1] \qquad \forall(d,l) \qquad (7d)$$

The weight function can be computed using a generalized SIMP scheme as

$$w(\boldsymbol{x},\boldsymbol{\rho}) = \rho_{dl}^{q}\, x_{plc}^{q} \qquad (8)$$

or a generalized RAMP scheme as

$$w(\boldsymbol{x},\boldsymbol{\rho}) = \frac{\rho_{dl}}{1 + q(1 - \rho_{dl})} \frac{x_{plc}}{1 + q(1 - x_{plc})} \qquad (9)$$

For simplicity, the same penalization factor q is applied for material design variables x_{plc} and density variables ρ_{dl}. The resulting parameterization is non-convex and therefore the solutions obtained are typically local optima. In order to prevent holes to appear inside the laminated structure, i.e. interior layers with zero density, a number of explicit constraints must be added. If the bottom layer $l = 1$ must have full density, i.e. be present, a series of constraints of the form $\rho_{dl} \geq \rho_{d(l+1)}$ are added as described in Sørensen and Lund (2013) and Sørensen et al. (2014) where a number of other manufacturing constraints also are described.

If all density variables ρ_{dl} can vary freely during the optimization, the constraints $\rho_{dl} \geq \rho_{d(l+1)}$ are not sufficient for forcing the optimization algorithm to yield a 0/1 solution. Two different approaches have successfully been applied for circumventing this problem, either using a dedicated move limit strategy or a thickness filter approach as developed in Sørensen and Lund (2015). In this work the move limit strategy described in Sørensen and Lund (2013) and Sørensen et al. (2014) combined with a Sequential Linear Programming (SLP) approach is documented. Basically, in each iteration the following constraints are applied

$$\rho_{d(l+1)} \leq f(\rho_{dl}, T), \quad \forall d,\ l = 1, 2, \ldots, n^l - 1 \tag{10}$$

Here $f(\rho_{dl}, T)$ is a function that controls the limit on the density variable of the contiguous upper layer based upon the current value of the density variable below and a threshold parameter T which is set to 0.1. The function $f(\rho_{dl}, T)$ is defined as

$$f(\rho_{dl}, T) = \begin{cases} f_1 = \frac{T}{1-T}\rho_{dl} & \text{if} \quad \rho_{dl} < (1-T) \\ f_2 = \frac{1-T}{T}\rho_{dl} + \frac{2T-1}{T} & \text{else} \end{cases} \tag{11}$$

The function $f(\rho_{dl}, T)$ is illustrated in Figure 3. With these modified constraints on the density variables, it is possible to avoid interior holes and obtain 0/1 solutions with the DMTO parameterization. The use of geometry design domains with the same thickness parameterization regularizes the thickness optimization problem and thereby removes the mesh dependence. Adding ply-drop constraints in the form of allowable rate of thickness variation between geometry domains also regularizes the optimization problem.

A number of manufacturing constraints can be considered in the DMTO approach as described in Sørensen and Lund (2013) and Sørensen et al. (2014). For constant thickness laminates symmetric laminates can be enforced in the DMO approach, see e.g. Yan et al. (2017) where other design guidelines like the 10% rule, etc., are taken into account. For the DMTO approach applied in this paper the thickness is reduced from the upper layer, such that it mimics the typical manufacturing process of, e.g., wind turbine blades where the fiber mats are placed in a single sided mould, and the tapering is performed on the outer layers. Enforcing symmetry around the midplane according to the current thickness of the laminated composite is not possible during the optimization process with the applied DMTO approach, and thus symmetric laminates are not enforced by the optimization procedure. This might be considered a disadvantage compared to many existing bi-level optimization procedures for monolithic laminates where symmetric laminates are enforced in the parameterization. However, with the DMTO approach multi-material laminates with varying thickness can be optimized, and as it will demonstrated by numerical examples in this paper, the DMTO approach very often yields nearly symmetric layups as solution to the optimization problem as such layups minimize extension-bending couplings and yield better structural performance.

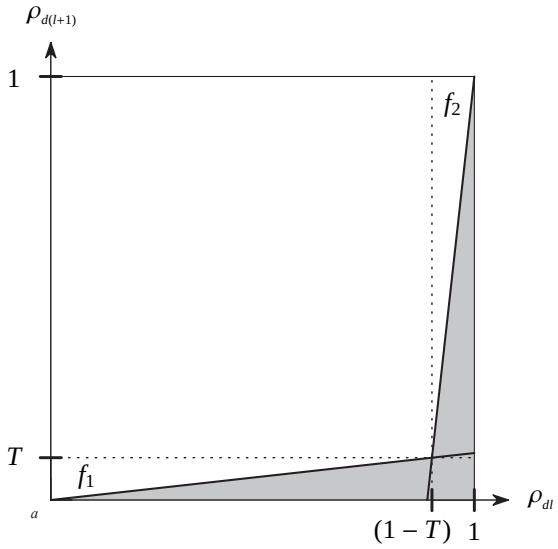

Figure 3: Illustration of function $f(\rho_{dl}, T)$ applied for preventing voids inside the laminate.

3 Failure analysis

The prediction of failure for the laminated composite structure is based on linear static stress analysis, and for simplicity only one load case is considered in the following, even though most practical design cases should take several load cases into account. The analysis is performed using Equivalent Single Layer (ESL) 9-node isoparametric shell finite elements, and the linear elastic static problem is solved for displacements $\boldsymbol{D}$ using the equilibrium equation

$$\boldsymbol{K}\boldsymbol{D} = \boldsymbol{F} \tag{12}$$

$\boldsymbol{F}$ is the global load vector and the global stiffness matrix $\boldsymbol{K}$ is determined as

$$\begin{aligned} \boldsymbol{K} &= \sum_{p=1}^{n^p} \sum_{e \in \mathcal{P}_p} \boldsymbol{K}_e \\ &= \sum_{p=1}^{n^p} \sum_{e \in \mathcal{P}_p} \sum_{l=1}^{n^l} \int_{\Omega_{el}} \boldsymbol{B}_{el}^T \boldsymbol{E}_{el} \boldsymbol{B}_{el} d\Omega_{el} \end{aligned} \tag{13}$$

Here summation denotes assembly of the local element stiffness matrices $\boldsymbol{K}_e$ where element e belongs to the list of elements, $\mathcal{P}_p$, for patch p. $\boldsymbol{E}_{el}$ is the effective constitutive matrix for layer l in element e, and $\boldsymbol{B}_{el}$ is the standard strain-displacement matrix. When evaluating an element stiffness matrix, the effective constitutive properties for any

layer are determined using the SIMP or RAMP schemes in either Eq. 4, 5, 8 or Eq. 9 with weight functions w_k. In stiffness driven design, e.g. for compliance problems, the penalization factor q is set such that the constitutive properties are reduced for intermediate design variable values, i.e., a below-linear penalization is used to guide the optimizer to select discrete 0/1 valued design variables.

Next the strength of the laminated composite must be evaluated. The layered shell elements used for the analysis in general give good prediction of inplane stresses in the laminated composite with linear variation within each layer. Due to the first order shear deformation theory applied, constant transverse shear stresses are obtained for each layer, whereas no information is available about transverse normal stresses. Thus, the prediction of strength using such layered shell elements in general is acceptable, but local effects from edges, ply drops, etc., can not be captured with these elements and thereby by the models applied in this work. However, the procedure described in this paper has also been implemented using solid shell elements, such that more detailed models can be applied, for example in combination with adaptive remeshing of zones of interest as documented in Johansen and Lund (2009) and Johansen et al. (2009).

The candidate materials will initially have equal design variables and thereby equal weight functions, and a relaxed effective failure index $FI_{eff,el}$ for each layer l of element e must be establish. The failure criteria used for FRP materials are evaluated in the material coordinate system 123, and based on the associated volume fraction of each candidate material, an effective failure index is computed. The approach follows the idea of Bruggi (2008) for stress constrained topology optimization, such that suitable penalization parameters different than those used for evaluating stiffness are used when evaluating the effective failure index.

The element strain vector $\boldsymbol{\epsilon}_{el}^{xyz}$ in the structural coordinate system is computed at both the bottom and top of each layer using

$$\boldsymbol{\epsilon}_{el}^{xyz} = \boldsymbol{B}_{el}\boldsymbol{d} \tag{14}$$

where $\boldsymbol{d}$ is the element displacement vector.

In case of having a stress-based failure criterion, the element layer stress vector $\boldsymbol{\sigma}_{el}^{xyz}$ is computed at the bottom and top of each layer as

$$\boldsymbol{\sigma}_{el}^{xyz} = \boldsymbol{E}_{el}\boldsymbol{\epsilon}_{el}^{xyz} \tag{15}$$

The strength prediction of candidate materials may be evaluated using different stress- or strain-based failure criteria, and thus stresses should vary in the same way as strains as function of design variables. Thus, the weight functions w_σ used for computing $\boldsymbol{E}_{el}$ in Eq. 15 are linear functions, such that no penalization of stresses is obtained. In this way strain- and stress-based failure criteria can be combined and penalized consistently.

For each candidate material c of the given layer, the strain vector $\boldsymbol{\epsilon}_{el}^{xyz}$ and stress vector $\boldsymbol{\sigma}_{el}^{xyz}$ are transformed to the material coordinate system 123 of the candidate material using appropriate standard transformation matrices, such that strain vector $\boldsymbol{\epsilon}_{elc}^{123}$ and stress vector $\boldsymbol{\sigma}_{elc}^{123}$ are obtained. For each candidate material a failure index FI_{elc} is evaluated using the preferred strain- or stress-based failure criteria. A number of different failure criteria have been implemented. This includes failure criteria not associated with failure modes like Tsai-Wu and Tsai-Hill together with criteria associated with failure modes. Here the two non-interactive criteria maximum strain and maximum stress are implemented together with the interactive Puck, LaRC 2-D and LaRC 3-D criteria. For simplification only maximum strain and maximum stress failure criteria are used for the examples in this work. Definitions of these criteria can be found in, e.g. Gürdal et al. (1999), and the result is a failure index FI_{elc} that must be ≤ 1 in order to avoid failure.

When failure indices FI_{elc} have been computed for each of the candidate materials, a resulting effective failure index $FI_{eff,el}$ is evaluated using

$$FI_{eff,el} = \sum_{c=1}^{n^c} w_{FI} FI_{elc} \tag{16}$$

The weight functions w_{FI} used for interpolation between failure indices for the different candidate materials must make it unfavorable to have intermediate design variable values, i.e. a linear or above-linear interpolation is applied. Using an above-linear interpolation the effective failure index is increased for intermediate design variable values, making such values disproportionately expensive. Furthermore, combined with the below-linear interpolation applied for w_k this yields the desired relaxation of stress based failure criteria, such that the contribution to $FI_{eff,el}$ approaches 0 as function of a design variable approaching 0. This might not be the case if $w_k = w_{FI}$.

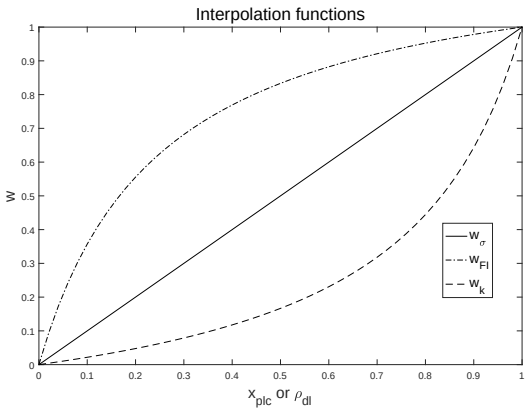

Figure 4: Typical choice of interpolation functions w_k, w_σ, and w_{FI} using the generalized RAMP scheme.

The main difference between using generalized SIMP and RAMP is that RAMP has a finite gradient for a design variable of value 0. For a SIMP scheme, see Eqs. 4 and 8, the derivative goes to infinity when a design variable approaches 0 and $0 < q < 1$ in order to obtain an above-linear interpolation. Thereby a positive lower bound on the design variable must be used for SIMP. For the RAMP scheme a lower bound of 0 can be applied for the design variables, which is an advantage of RAMP. Therefore all results presented in this work are based on the RAMP scheme, but quite similar results are obtained with the SIMP scheme when having a small positive lower limit

on the design variables. A typical choice of the weight functions w_k, w_σ, and w_{FI} using the generalized RAMP scheme is illustrated by Figure 4. The values applied for the penalization power q are described in detail in the following section.

4 Optimization approach

Having established the parameterization and failure analysis approach, the optimization problem to be solved can be established and solved using standard mathematical programming techniques.

4.1 Design sensitivity analysis and SLP approach

The computation of gradients has been implemented using both analytical and semi-analytical approaches based on direct differentiation and adjoint methods. Details for these methods of design sensitivity analysis can be found in e.g. Haftka and Gürdal (1992) and Tortorelli and Michaleris (1994). Failure criteria not associated with failure modes like Tsai-Wu and Tsai-Hill are continuous and differentiable functions, so the computation of gradients of failure indices can be performed as described in e.g. Groenwold and Haftka (2006). The failure criteria used in the examples in this paper are all associated with failure modes, like the non-interactive maximum strain and maximum stress criteria. Thus, the failure surfaces are continuous but have nondifferentiable points at the intersection between surfaces associated with the different failure modes. In practice, it is very rare that such points are reached in the evaluation of failure indices, and for the gradient evaluation, the sensitivity is computed assuming fixed failure mode. For example, if the analysis predicts failure due to compressive transverse inplane stress in the material coordinate system, then the sensitivity of the failure index is computed for this failure mode.

The optimization problems are solved using SLP as described in detail in Sørensen and Lund (2013) and Sørensen et al. (2014). The DMO and DMTO parameterizations introduce a very large number of sparse linear constraints, see Eqs. 3b and 7b, and thus it is an advantage to use an optimizer that has good support for such sparse constraints. In this work the LP optimizers in IBM ILOG CPLEX version 12.6, see IBM ILOG (2015), and version 7.2-9 of the Sparse Nonlinear OPTimizer (SNOPT) by Gill et al. (2005) have been applied, both with default settings.

The presented approach results in a very large number of failure indices that must be taken into account. For a finite element model consisting of n^e elements, each with n^l layers, the number of failure indices is $2 \cdot n^e \cdot n^l$. Combined with the large number of design variables needed for the DMO and DMTO approach, it is necessary from a computational point of view to cluster a large number of the local failure indices into a lower number of global values. A number of different aggregate functions have been implemented including P-norm, P-mean-norm and Kreisselmeier-Steinhauser functions. For simplicity, only results obtained using the P-norm function are presented. If the failure indices to include are stored as FI_k, $k = 1, \ldots, n^{FI}$, then the P-norm function FI_{PN} is computed as

$$FI_{PN} = \left(\sum_{k=1}^{n_{FI}} (FI_k)^P \right)^{1/P} \tag{17}$$

The parameter P controls the level of smoothness, and the P-norm value approaches the value of the largest failure index from above as $P \to \infty$. Thus, it is desirable to select a large value of P, but it also makes the optimization problem increasingly non-linear and more difficult to solve. In this work a value of 8 is used for P in all examples.

A number of different approaches for determining the failure indices to include in the optimization problem have been implemented in this work. Some approaches are purely based on sorting all failure indices, like including a fixed number of the largest values or active set strategies where values exceeding a given percentage of the largest value are included. Other approaches are related to the material and geometry patches introduced with the parameterization, such that values from all patches are included in the aggregate function. For all examples presented it is specified how the failure indices FI_k are extracted from the full set of values.

The efficiency of using global strength approaches decreases when a large number of values are lumped into a single global value, but this problem can be handled by associating a global strength measure with each material/geometry patch used for the parameterization. The approach then has similarities with the block aggregation approach París et al. (2010) and the regional stress measure approach Le et al. (2010) used for single-material structural topology optimization problems with stress constraints.

In case of having failure indices as objective function, i.e. solving problems with minimizing the maximum failure index, the P-norm overestimation of the largest failure index value in general is not a problem. However, when failure indices are included as constraints, the overestimation typically results in a design where the true failure index constraint is not active. This is solved using the adaptive constraint scaling scheme proposed in Le et al. (2010). With this approach the constraint is scaled according to the ratio of the current maximum failure index value and the P-norm value together with history information about the constraint scaling, see details about our implementation in Oest and Lund (2017). This adaptive constraint scaling scheme has the advantage that lower values of P can be applied, which makes the optimization problem easier to solve.

The computational cost of including strength criteria in the optimization problem is comparable to include buckling constraints, i.e. it is computationally much more intensive than solving compliance problems. Quite often stiffness is used as a surrogate objective function for obtaining a high strength design, but the difference between strength and stiffness optimized designs may be significant as illustrated by several examples in IJsselmuiden et al. (2008). Their results clearly indicate that the degree of correlation between stiffness and strength driven designs of laminates depends on the properties of the materials and the loading situation.

4.2 Continuation approach

All numerical examples shown in Section 5 are solved using a continuation approach for the generalized RAMP scheme. Due to the non-convexity of the optimization problem, any gradient based optimization approach is likely to end in a local minimum. Even for stiffness topology optimization problems using a single isotropic material and the SIMP interpolation, a continuation approach may help in obtaining a strong local minimum because the stiffness penalized problem is non-convex. This is illustrated in the recent paper by Aage et al. (2017) where a 3D compliance optimization problem with more than 1 billion design variables is solved. They had to slowly raise the SIMP penalization power in steps of 0.25 from 1 to 3, distributed over a total of 400 design iterations, in order to obtain a strong local minimum. The same observations are made for the density approach in this paper. Starting the optimization problems with high penalization parameters will quickly force the design to a sub-optimal 0/1 solution. Applying a continuation scheme results in more design iterations but better solutions. The sensitivity to choice of penalization parameters for the presented approach seems to be similar to the sensitivity observed for standard topology optimization problems using a density approach.

In general, best results will be obtained by keeping the values of q fixed until convergence in design variables, before their values are increased in the continuation approach, but this may yield quite many iterations. Therefore the values of q are updated after a fixed number of iterations. This will be specified in the numerical examples (it is typically 10-30). If the convergence criterion applied is fulfilled before the final continuation step, then the q parameter is increased, such that the final continuation values of q always are applied.

The values used for the penalization parameter q in the continuation approach are listed in Table 1. Values of q used for interpolation of mass, mass matrix for eigenfrequency analysis, and stress stiffness matrix applied for linear buckling analysis are also given. These values of q represent a good trade-off between computational cost and quality of the solution obtained. The optimization problems are always initialized with equal weighting of the candidate materials as the optimization procedure otherwise typically converge to a local minimum.

Table 1: Continuation approach used for RAMP scheme.

Weight function	Values of q	Applied for
w_k	1, 4, 20	Stiffness matrix
w_σ	0	Stresses
w_{FI}	0, -0.4, -0.8	Failure indices
w_m	0	Mass and mass matrix
w_{k_σ}	1, 4, 20	Stress stiffness matrix

The convergence criterion of having a relative change in design variables less than 0.1% is applied for all examples. In order to measure the obtained level of discreteness of the design variables, two measures of non-discreteness are computed. The measure of density non-discreteness is calculated as suggested by Sigmund (2007) as

$$M_{dnd} = \frac{4 \sum_{d,l} V_{el}\, \rho_{el}\, (1 - \tilde{\rho}_{el})}{\sum_{d,l} V_{el}} \cdot 100\% \qquad (18)$$

where V_{el} is the layer volume of the e'th element. The measure of candidate non-discreteness is calculated according to Sørensen et al. (2014), and repeated here for completeness

$$M_{cnd} = \frac{\sum_{e,l} V_{el}\, \tilde{\rho}_{el}^2 \prod_{c=1}^{n^c} \left(\frac{1 - x_{plc}}{1 - \frac{1}{n^c}} \right)^2}{\sum_{e,l} V_{el}\, \tilde{\rho}_{el}} \cdot 100\% \qquad (19)$$

5 Numerical examples

In the following a series of numerical examples are presented. The material properties used for all examples are given by Table 2. The candidate materials include glass-epoxy (GFRP) UD material, glass-epoxy biax material (cross-ply), and PVC H130 foam.

Table 2: Properties of UD GFRP, biax GFRP and PVC H130 foam material (ESAComp, 2016)

Property	Units	UD	Biax	PVC 130
Young's modulus E_{11}	[GPa]	38.0	24.0	0.148
Young's modulus E_{22}	[GPa]	9.0	24.0	-
Shear modulus G_{12}	[GPa]	3.6	3.6	-
Shear modulus G_{23}	[GPa]	3.46	3.5	-
Shear modulus G_{13}	[GPa]	3.6	3.5	-
Poisson's ratio ν_{12}	-	0.30	0.11	0.45
Density ϱ	[kg/m^3]	1870	1870	130
Long. tensile strength X_t	[MPa]	930	84	4.8
Long. compressive strength X_c	[MPa]	570	260	3.0
Transv. tensile strength Y_t	[MPa]	33	84	-
Transv. compressive strength Y_c	[MPa]	110	260	-
In-plane (12) shear strength S_{12}	[MPa]	70	60	2.2
Trans. (13) shear strength S_{13}	[MPa]	70	35	-
Trans. (23) shear strength S_{23}	[MPa]	42	35	-
Long. tensile strain ϵ_{1t}	[%]	2.45	0.35	3.24
Long. compressive strain ϵ_{1c}	[%]	1.5	1.08	2.03
Transv. tensile strain ϵ_{2t}	[%]	0.37	0.35	-
Transv. compressive strain ϵ_{2c}	[%]	1.22	1.08	-
In-plane (12) shear strain γ_{12u}	[%]	1.94	1.66	4.4
Transv. (13) shear strain γ_{13u}	[%]	1.94	1.0	-
Transv. (23) shear strain γ_{23u}	[%]	1.2	1.0	-

5.1 Fiber angle optimization of clamped single-layer square plate with uniform pressure

The first example illustrates how fiber angle optimization of a clamped single-layer square plate with uniform pressure can be performed. This example is a standard test example where symmetric fiber angle distributions are expected for the optimized solution, and as such it is a very good benchmark example for testing the performance for difference material parameterizations, i.e. DMO material

patches. Manufacturability is not considered for this benchmark problem. The problem is defined by Figure 5. The candidate materials are GFRP UD with $-45°$, $0°$, $45°$, and $90°$ fiber orientations, and the objective is to minimize the maximum failure index in the plate.

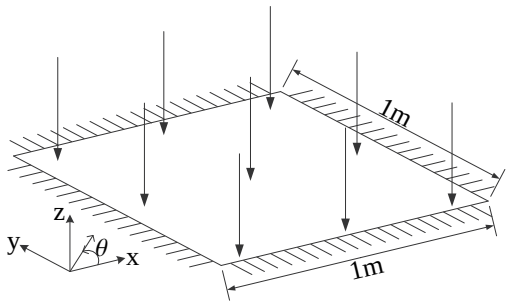

Figure 5: Illustration of the clamped single-layer square plate. The plate is subjected to a uniform pressure at its upper surface with a magnitude of 1 MPa. The thickness of the plate is 0.04m.

The plate is discretized with 32 x 32 9-node isoparametric shell finite elements, and the example is solved for five different DMO material patches, where the plate is divided into 2x2, 4x4, 8x8, 16x16, and 32x32 material domains having the same fiber angle. Failure indices are computed at the bottom and top of each layer, such that a total number of 2,048 failure indices are computed. It is chosen to include the two largest values of each patch in the *P*-norm function used for computing the aggregated global strength measure. The number of failure criteria n_{FI} included thereby varies for each parameterization. The penalization parameter q varies according to Table 1, and it is changed after every 10 iterations. The optimization problem is solved using SLP using a 10% adaptive move limit strategy as described in Sørensen et al. (2014). The results obtained when failure indices are computed using the maximum strain failure criterion are presented in Table 3. In order to compare the DMO solutions with the fiber angle distribution obtained with continuous fiber angle optimization (CFAO), the 32x32 parameterization, i.e. when fiber angles can vary within each element, is also solved with CFAO.

Table 3: Tabular overview of results of all parameterizations for the single-layered clamped plate example when using the maximum strain failure criterion. The maximum failure index is for the final (rounded) 0/1 design. $\#It$ denotes the total number of iterations.

Parameterization	N_{FI}	$max\ FI$	M_{cnd} [%]	$\#It$
2 x 2 DMO patches	8	0.682	96.15	16
4 x 4 DMO patches	32	0.292	0.00	46
8 x 8 DMO patches	128	0.288	0.00	39
16 x 16 DMO patches	512	0.244	0.02	88
32 x 32 DMO patches	2048	0.235	0.07	152
Elementwise CFAO	2048	0.167	-	93

From Table 3 it is seen that most of the discretizations converge to a 0/1 solution, except for the 2 x 2 DMO patch problem which is simply parameterized too coarsely. This optimization problem fulfills the convergence criterion of having a relative change in design variables less than 0.1% after 16 iterations, even though the measure of candidate non-discreteness M_{cnd} is more than 96%. The maximum failure index listed in the examples is always computed for the (rounded) 0/1 design. In general, the number of iterations needed increases with the number of design variables. This is expected for such strength related optimization problems as they are much more difficult to solve than compliance problems.

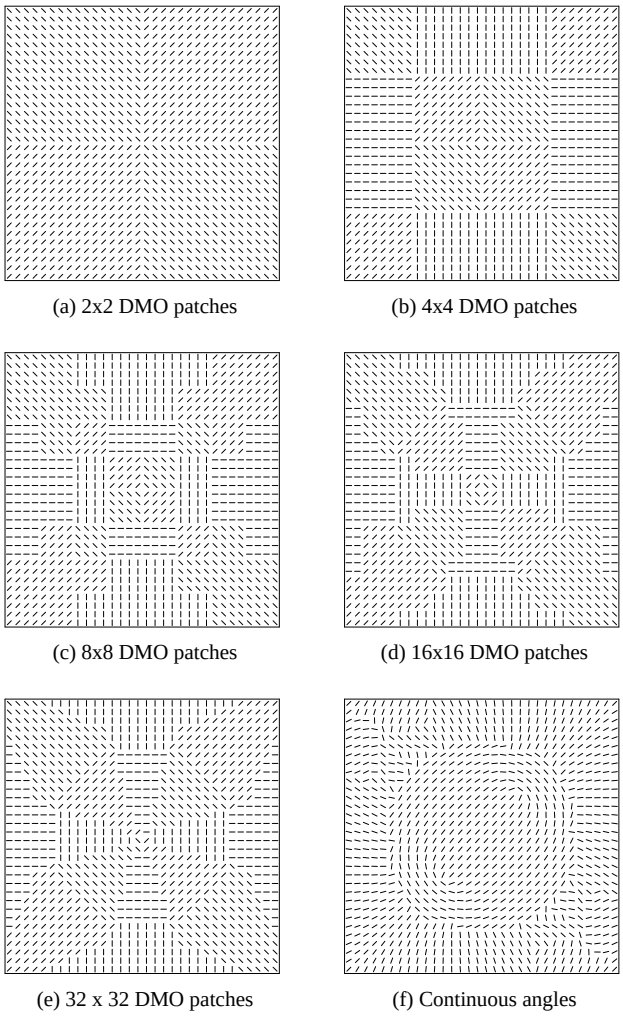

(a) 2x2 DMO patches (b) 4x4 DMO patches

(c) 8x8 DMO patches (d) 16x16 DMO patches

(e) 32 x 32 DMO patches (f) Continuous angles

Figure 6: Optimized fiber angle distributions for single-layer clamped plate examples. The FE model consists of 32 x 32 9-node shell elements.

The fiber angle distributions obtained are illustrated in Figure 6. Most of the DMO fiber angles are as expected, except for a few angles for the 32x32 patch model. One would expect symmetric solutions for this example as the four candidate angles have equal weighting initially, but due to the non-convexity of the problem a few angles converge to a local minimum. This is also demonstrated for the solution obtained using continuous fiber angles. The initial fiber angles are $0°$, and the solution obtained is definitely a local minimum. However, due to the larger design freedom with continuous fiber angles, the maximum failure index is lower than for the DMO solution. The distribution of failure

indices for the bottom of the optimized plates is shown in Figure 7. The fiber angle distributions in the corners of the plate are different from the classical analytical grillage solutions obtained in Rozvany (1972). This difference is expected to be due to the assumptions in the analytical grillage theory. The fiber angle distributions in the corners of the plate are similar, if the objective is to minimize compliance, whereas differences are seen in many other parts of the plate.

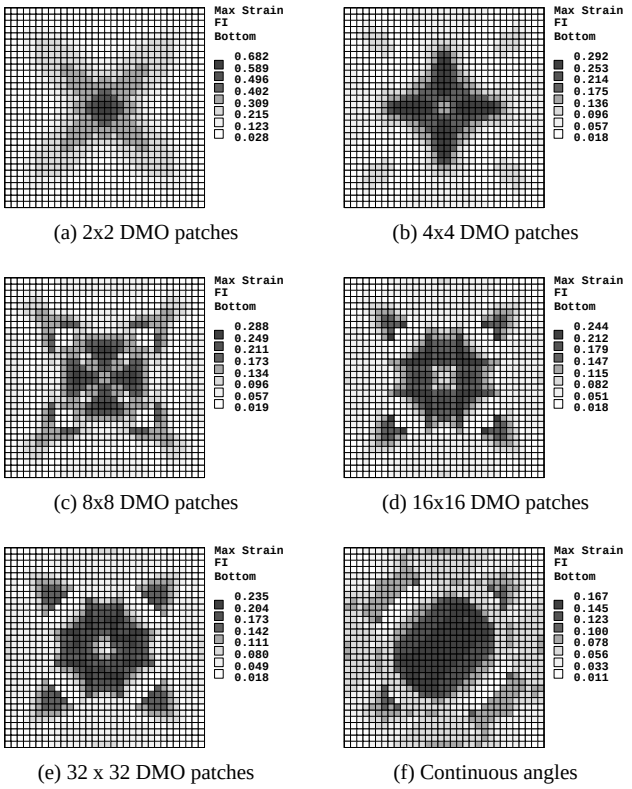

(a) 2x2 DMO patches (b) 4x4 DMO patches

(c) 8x8 DMO patches (d) 16x16 DMO patches

(e) 32 x 32 DMO patches (f) Continuous angles

Figure 7: Maximum strain failure index at bottom of optimized single-layer clamped plates.

A typical iteration history is shown in Figure 8 for the model with 16x16 DMO patches. The change of penalization power after iteration 10 and 20 is seen to cause a large increase in the failure index value, but the optimization algorithm converges to a distinct choice of fiber angles.

Next the same example is solved using the maximum stress failure criterion in order to document that both strain and stress based failure criteria can be applied. The results are shown in Table 4. In general, the results are very similar to the results obtained using the maximum strain failure criterion, except for the 8x8 patch parameterization that ends in a local minimum. For other choices of move limits, this problem can converge to the same fiber angle solution as shown in Figure 6 which again illustrates the non-convexity of the optimization problem. The sensitivity to move limit values for the SLP algorithm is similar to the sensitivity seen for other topology optimization problems. The move limits have to be sufficiently small, such that the linear approximations applied are sufficiently accurate. The number of iterations used is more or less the same for both criteria.

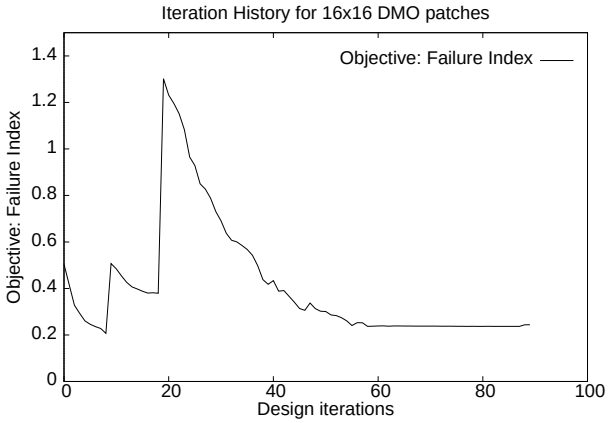

Figure 8: Iteration history for 16x16 DMO patch model when using the maximum strain failure index

Table 4: Tabular overview of DMO results of all parameterizations for the single-layered clamped plate example when using the maximum stress failure criterion.

Parameterization	N_{FI}	$max\ FI$	M_{cnd} [%]	$\#It$
2 x 2 DMO patches	8	0.778	96.11	20
4 x 4 DMO patches	32	0.327	0.00	30
8 x 8 DMO patches	128	0.343	0.02	45
16 x 16 DMO patches	512	0.305	0.02	65
32 x 32 DMO patches	2048	0.277	0.03	131

These examples have also been solved using the generalized SIMP scheme with a lower limit of 10^{-4} on the design variables, and the results and performance are quite similar to the above results obtained with generalized RAMP.

5.2 Five-layer cantilever beam

The remaining examples illustrate the performance of the DMTO approach, i.e. simultaneous determination of thickness variation and material distribution. The first example is another benchmark example as the solutions can be verified by exhaustive search. Again, manufacturability is not considered for this benchmark problem. The example is defined in Figure 9.

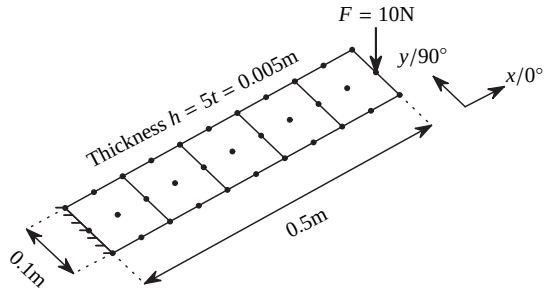

Figure 9: Five-layer cantilever beam subjected to load F = 10 N and discretized by five 9-node shell elements. Ply thickness t is 0.001 m.

The objective is to minimize the maximum failure index

of the five-layer GFRP cantilever beam, subject to the mass constraint that 15/25 of the domain can be occupied by material. Again the candidate materials are GFRP UD oriented at $-45°$, $0°$, $45°$, and $90°$, but now the same material should be selected for each layer, i.e. only one material patch is defined. The thickness can vary for each of the five geometry domains (here equal to the finite element discretization), however, slope constrains are added to the problem in order to limit the thickness changes. These slope constraints specify that the thickness can only increase by one layer between the geometry domains. Details about the linear inequalities used for specifying slope constraints can be found in Sørensen and Lund (2013) and Sørensen et al. (2014). The bottom layer must always exist, i.e. it has full density. The two largest failure indices of each geometry domain are included in the computation of the P-norm global failure index, such that 10 failure indices are included in total.

The result of the optimization is seen in Figure 10 (a) where layer thicknesses are scaled by a factor of 20. The problem is also solved with the additional constraint that no identical contiguous plies are allowed. This is a manufacturing rule used in many cases in order to avoid a number of layers with the same fiber angle, as this may result in a larger build-up of transverse stresses causing delamination. The formulation of such linear inequality constraints for specifying limits on contiguous plies can also be found in Sørensen and Lund (2013) and Sørensen et al. (2014). The result of this case is shown in Figure 10 (b). In both cases the starting design has full density of all layers, i.e. the starting point is infeasible, and the optimization problem is solved using the SLP approach described in Sørensen and Lund (2013) with 10% move limits. As in the previous example, the penalization parameter q varies according to Table 1 and is changed after every 10 iterations.

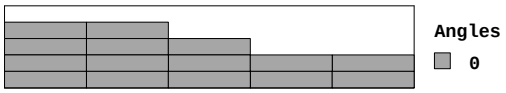

(a) DMTO design with ply drop constraint

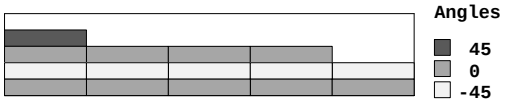

(b) DMTO design with ply drop constraint and no identical contiguous plies allowed

Figure 10: Optimized fiber angle and thickness distributions for five-layer cantilever beam example. The thicknesses are scaled by a factor of 20.

The solutions are found after 31 and 52 iterations, respectively, and in both cases full convergence is obtained, i.e. $M_{dnd} = M_{cnd} = 0.0\%$. The two solutions shown agree with the global integer optimum determined by exhaustive search. For the second case, the $+45°$ and $-45°$ candidate angles are equally good to select due to symmetry, so the material choice for layer 2 and 4 can be interchanged with the same result for the computed failure index.

It should be noted that the DMTO parameterization yields exterior ply drops which in general should be avoided when designing varying thickness laminates, see e.g. Cairns et al. (1999) and Mukherjee and Varughese (2001). However, it is outside the scope of this paper to present DMTO parameterizations aimed at generating interior ply drops, as the main objective is to present the inclusion of strength criteria in existing DMO and DMTO parameterizations.

5.3 Corner hinged eight-layer plate

Next a corner hinged eight-layer GFRP plate is considered.

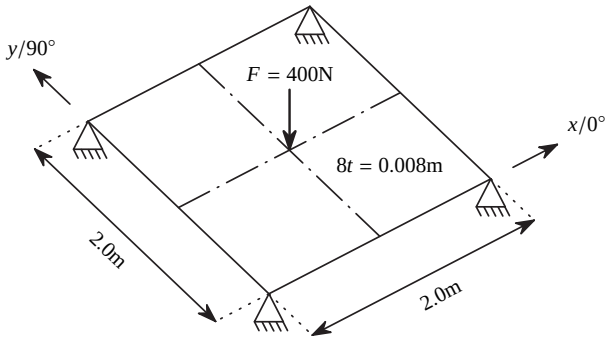

Figure 11: Corner hinged eight-layer plate. Ply thickness is 0.001 m.

The objective is to minimize the maximum failure index of the eight-layer GFRP plate, subject to the mass constraint that half of the domain can be filled with material. The bottom layer must exist, i.e. it has full density, and the material choice should be the same for each layer in order to ease manufacturability. It should be noted that the DMTO parameterization applied results in exterior ply drops, which in general should be avoided due to risk of delamination. Thus, an improved DMTO parameterization would be useful, if the optimized design should directly be ready for manufacturing. However, the main aim of this paper is to document the possibility of including failure criteria for the multi-material density approach, and the development of an improved DMTO parameterization is left for future work. As in the previous examples the candidate materials are GFRP UD with $-45°$, $0°$, $45°$, and $90°$ fiber orientations, and for the thickness parameterization 24x24 geometry domains are defined. The plate is discretized with a 48 x 48 mesh of 9-node shell elements, such that each geometry domain consists of 2x2 elements. Four contiguous identical layers are allowed, and slope constraints are specified, such that the layer thickness can only change by one layer between geometry domains. In total the problem has 36,864 potential failure indices computed using the maximum strain criterion and 1,041 design variables. Failure indices exceeding 50% of the largest failure index in a given iteration are included in the computation of the P-norm global failure index, taking the conditions into account that at least 300 values and at most 1000 failure index values are included.

Again all layers have full density for the initial design, such that the starting point is infeasible. The penalization parameter q varies according to Table 1 and is changed after every 30 iterations. A 10% move limit is applied.

The problem needs 58 iterations before the convergence criterion is fulfilled. The choice of material is distinct, i.e. $M_{cnd} = 0.0\%$, while the measure of density non-discreteness is $M_{dnd} = 3.1\%$. The mass constraint is active for the optimized design, and with the parameterization applied combined with the value of the mass constraint, a couple of geometry domains do not obtain a distinct number of layers. Results are shown for a rounded 0/1 design. In this case the mass constraint is accidently still fulfilled for the rounded design, but this is in general not the case using simple rounding.

The choice of fiber angle and thickness distribution of the final design is illustrated using a solid model in Figure 12 where thicknesses are scaled by a factor of 20.

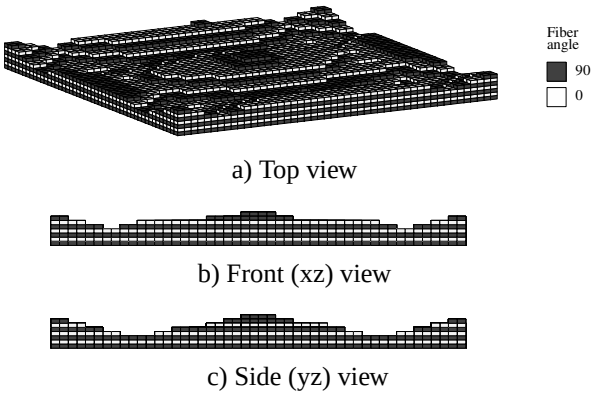

Figure 12: Optimized design of corner hinged eight-layer plate.

The solution resembles a cross ply laminate with varying thickness, except that 90° has been selected for both layer 7 and 8. A slight asymmetry is introduced which is expected to be due to the mass constraint. Note that the layup is symmetric, except for the fiber angle chosen for the small amount of material in the upper layer 8. Thus, even though a symmetric layup is not enforced by the parameterization, the optimization approach yields such a layup with high performance.

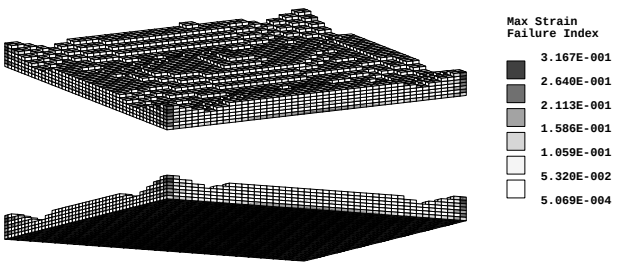

Figure 13: Failure index distribution for optimized design of corner hinged eight-layer plate.

The maximum strain failure index of the final design is illustrated in Figure 13, again using a solid model where thicknesses are scaled by a factor of 20. A quite uniform distribution of the failure indices is seen, taking into account that the same fiber angle must be chosen for each layer.

5.4 Multi-criteria optimization of main spar from wind turbine blade

The final study is related to a complex multi-criteria optimization example of designing a simplified main spar from a wind turbine blade. It was studied in detail for the DMTO formulation in Sørensen et al. (2014), and here the example is extended with the inclusion of strength constraints. It is outside the scope of this paper to describe the example in detail, as it is mainly included in order to demonstrate the behaviour of the optimization process when many different structural criteria are included.

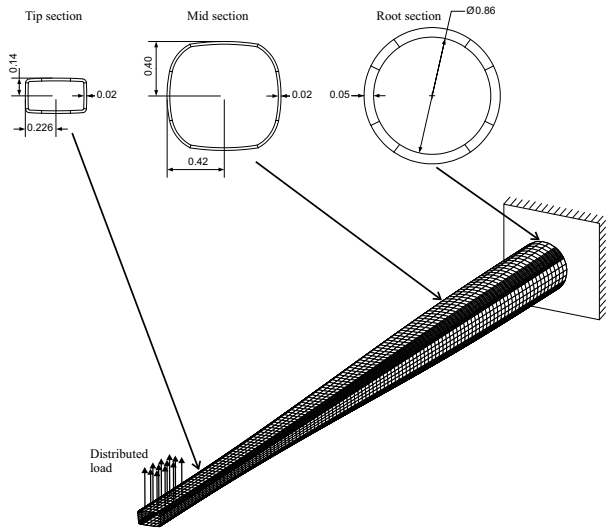

Figure 14: Simplified model of main spar from wind turbine blade.

The geometry of the 25 m simplified main spar is shown in Figure 14. The model is clamped at the circular root end and the applied loads resemble the most critical extreme flapwise bending situation, happening in a so-called 50 year gust scenario. The loads are taken from experimental tests of the real wind turbine blade and are applied as a distributed load, corresponding to a resulting load of 164.7 kN, see details in Overgaard et al. (2010). The finite element model consists of 7,168 9-node shell elements with 20 layers everywhere. The inner geometry of the main spar is used as reference, and ply thickness of each of the 20 layers is 0.0025 m, resulting in a maximum total laminate thickness of 0.05 m. A total number of 448 patches are applied for parameterization of both material and thickness. Six different candidate materials commonly applied in the wind turbine industry are defined. The first four candidates represent GFRP UD plies with $-45°$, $0°$, $45°$, and $90°$ fiber orientations relative to the axial direction of the main spar. The 5th candidate represents a GRFP biax ply and the last candidate represents a lightweight isotropic foam material such that a sandwich structure is a possible outcome of the optimization problem. The problem thereby involves 62,720 design variables.

The objective is to minimize mass while fulfilling a number of structural constraints. The lowest linear buckling load factor must be ≥ 3 and the lowest eigenfrequency must be ≥ 1 Hz. For both eigenvalue criteria the five lowest

values are included in the optimization problem. The tip displacement must be ≤ 1 m and the failure indices must be ≤ 1. The total number of failure indices is 286,720 failure indices which are reduced to 448 constraints using P-norm functions, each consisting of the 10 largest failure index values within each patch. Finally, a maximum number of 8 consecutive identical layers are allowed, and ply drop constraints enforce that thickness changes between patches is limited to the thickness of one layer.

The problem is solved with 10% move limits and the q values are updated according to Table 1 for every 30 iterations. The iteration history is given by Figure 15. The convergence criterion is fulfilled after 87 iterations, where the measure of candidate non-discreteness is $M_{cnd} = 0.13\%$ and the measure of density non-discreteness is $M_{dnd} = 0.20\%$. Thus, the optimized solution is very close to a pure 0/1 design.

The lowest linear buckling load factor is 3.02, the tip displacement is 1.00 m, and the maximum failure index is 0.99, i.e. these three constraints are at or very close to their allowable values. The lowest eigenfrequency is 3.38 Hz and it is never active during the optimization process. The structural criteria are conflicting in the sense, that the buckling load factor will be increased by having several layers at the top and bottom of the main spar with $-45°$, $45°$, and $90°$ fiber orientations, whereas the $0°$ fiber angle (axial direction) will be the main preferred choice for the other structural criteria. Thus, the distribution of fiber angles and thicknesses is a tradeoff between conflicting criteria, and it is quite similar to the design presented in Sørensen et al. (2014), except that the mass is increased by approximately 100 kg to 1273 kg when failure criteria are included in the optimization problem. Thus, the distribution of fiber angles and thicknesses of the 448 design domains with up to 20 layers is not shown here due to the similarities with the design presented in detail in Sørensen et al. (2014).

The iteration history given by Figure 15 illustrates how the failure criterion constraint increases significantly when the q penalization parameter is changed after 30 iterations. Subsequently, the mass is increased in order to obtain a feasible solution, and most of the design variables have converged after 60 iterations when the q parameter is changed to its final value. This multi-criteria design optimization problem illustrates that failure criteria can be successfully included in complicated laminated composite design problems with conflicting structural criteria.

6 Conclusions

In this paper the DMO and DMTO parameterization approches for optimization of laminated composite structures have been extended to include failure criteria. The interpolation schemes are multi-material variations of the well-known SIMP and RAMP interpolation schemes where suitable penalization parameters are applied. Thus, the work can be considered as an extension of stress constrained topology optimization of single-material problems to multi-material problems. The large number of local constraints is reduced by the use of aggregate functions, and four different design optimization problems have demonstrated the efficiency of the approach. This includes minimization of the maximum failure index in single- and multi-layer plate examples, and a challenging example of mass minimization of a main spar from a wind turbine blade, taking strength, buckling load factors, eigenfrequency and displacement constraints into account.

The DMTO parameterization applied results in exterior ply drops, that produce internal and local stress concentrations not captured by the shell finite elements applied as a consequence of geometric discontinuities and shear lag. Factors that effect the performance of laminated composite structures with ply drops include thicknesses, ply stacking sequences, ply drop geometries and manufacturing considerations, and a continuation of the work presented in this paper would be to develop an improved DMTO parameterization that can generate interior ply drops with improved strength performance. The DMTO approach is still a tool to be applied in the conceptual design phase as postprocessing is needed for the final manufacturable design.

Acknowledgements

This work was partly supported by the Danish Research Council for Technology and Production Sciences (FTP), grant no. 10-082695, and the Innovation Fund Denmark project OPTI_MADE_BLADE, grant no. 75-2014-3. This support is gratefully acknowledged.

References

Aage, N., E. Andreassen, B. S. Lazarov, and O. Sigmund (2017). Giga-voxel computational morphogenesis for structural design. *Nature 550*(7674), 84–86.

Bendsøe, M. P. (1989). Optimal shape design as a material distribution problem. *Structural Optimization 1*(4), 193–203.

Blasques, J. P. and M. Stolpe (2012). Multi-material topology optimization of laminated composite beam cross sections. *Composiste Structures 94*(11), 3278–3289.

Bloomfield, M. W., C. G. Diaconu, and P. M. Weaver (2009, apr). On feasible regions of lamination parameters for lay-up optimization of laminated composites. *Proceedings of the Royal Society A: Mathematical, Physical and Engineering Science 465*(2104), 1123–1143.

Bruggi, M. (2008). On an alternative approach to stress constraints relaxation in topology optimization. *Structural and Multidisciplinary Optimization 36*(2), 125–141.

Bruyneel, M. (2011, jan). SFP-a new parameterization based on shape functions for optimal material selection: application to conventional composite plies. *Structural and Multidisciplinary Optimization 43*(1), 17–27.

Bruyneel, M. and P. Duysinx (2006). Note on singular optima in laminate design problems. *Structural and Multidisciplinary Optimization 31*(2), 156–159.

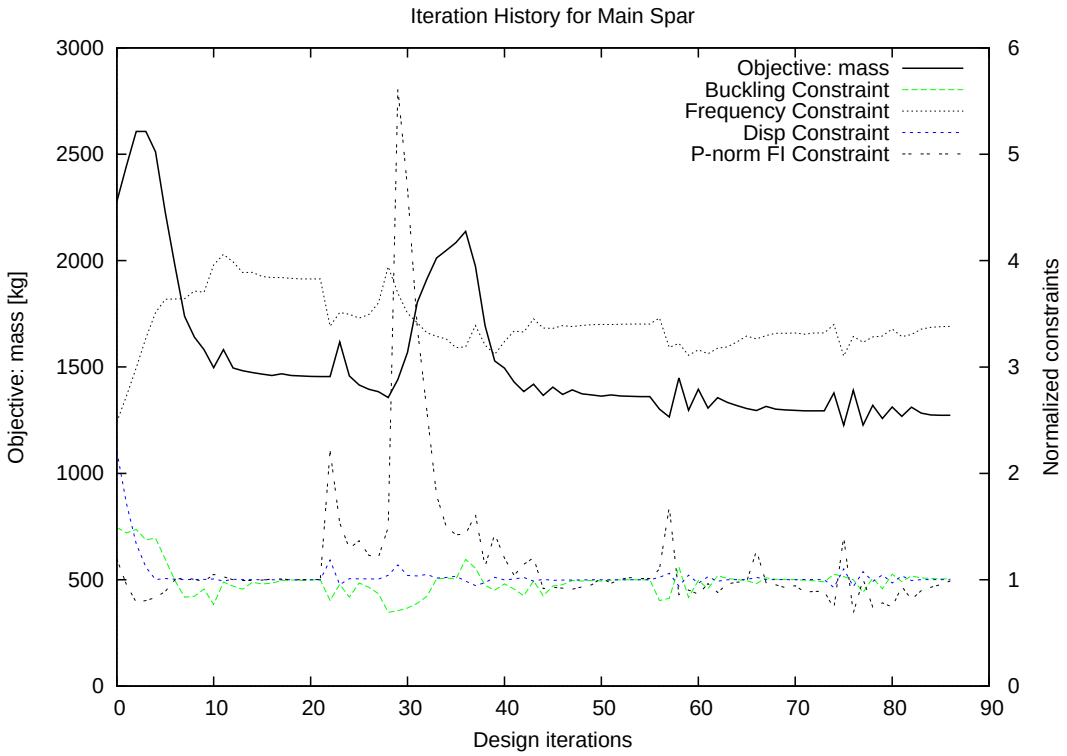

Figure 15: Iteration history

Bruyneel, M., P. Duysinx, C. Fleury, and T. Gao (2011). Extensions of the Shape Functions with Penalization Parameterization for Composite-Ply Optimization. *AIAA Journal 49*(10), 2325–2329.

Cairns, D., J. Mandell, M. Scott, and J. Maccagnano (1999, jul). Design and manufacturing considerations for ply drops in composite structures. *Composites Part B: Engineering 30*(5), 523–534.

Cheng, G. and N. Olhoff (1981). An investigation concerning optimal design of solid elastic plates. *International Journal of Solids and Structures 17*(3), 305–323.

Cheng, G. D. and X. Guo (1997). ϵ-relaxed approach in topology optimization. *Structural Optimization 13*, 258–266.

Cheng, G. D. and Z. Jiang (1992). Study on topology optimization with stress constraint. *Engineering Optimization 20*, 129–148.

Cheng, K. T. and N. Olhoff (1982). Regularized formulation for optimal design of axisymmetric plates. *International Journal of Solids and Structures 18*(2), 153–170.

de Faria, A. R. (2015). Optimization of composite structures under multiple load cases using a discrete approach based on lamination parameters. *International Journal for Numerical Methods in Engineering 104*(9), 827–843.

Duysinx, P. and M. P. Bendsøe (1998). Topology optimization of continuum structures with local stress constraints. *Int. Journal for Numerical Methods in Engineering 43*, 1453–1478.

Duysinx, P. and O. Sigmund (1998). New development in handling stress constraints in optimal material distribution. In *7th AIAA/USAF/NASA/ISSMO symposium on multidisciplinary analysis and optimization. A collection of technical papers (held in St. Louis, Missouri)*, Volume 3, pp. 1501–1509.

ESAComp (2016). *ESAComp - Software for Analysis and Design of Composites, Release 4.5.2, http://www.esacomp.com*.

Gao, T., W. Zhang, and P. Duysinx (2012). A bi-value coding parameterization scheme for the discrete optimal orientation design of the composite laminate. *International Journal for Numerical Methods in Engineering 91*(1), 98–114.

Ghiasi, H., K. Fayazbakhsh, D. Pasini, and L. Lessard (2010). Optimum stacking sequence design of composite materials Part II: Variable stiffness design. *Composite Structures 93*(1), 1–13.

Ghiasi, H., D. Pasini, and L. Lessard (2009). Optimum stacking sequence design of composite materials Part I: Constant stiffness design. *Composite Structures 90*(1), 1–11.

Gill, P. E., W. Murray, and M. A. Saunders (2005). SNOPT: An SQP algorithm for large-scale constrained optimization. *SIAM Review 47*(1), 99–131.

Groenwold, A. A. and R. T. Haftka (2006). Optimization with non-homogeneous failure criteria like {T}sai–{W}u for composite laminates. *Structural and Multidisciplinary Optimization 32*, 183–190.

Guo, X., G. D. Cheng, and K. Yamazaki (2001). A new approach for the solution of singular optima in truss topology optimization with stress and local buckling constraints. *Structural and Multidisciplinary Optimization 22*(5), 364–373.

Gürdal, Z., R. T. Haftka, and P. Hajela (1999). *Design and Optimization of Laminated Composite Materials*. New York: John Wiley & Sons.

Gürdal, Z., R. T. Haftka, and S. Nagendra (1994). Genetic Algorithms for the design of laminated composite panel. *Mechanics of Advanced Materials and Structures 30*(3), 29–35.

Haftka, R. T. and Z. Gürdal (1992). *Elements of Structural Optimization* (3 ed.). Kluwer.

Hammer, V. B., M. P. Bendsøe, R. Lipton, and P. Pedersen (1997). Parametrization in laminate design for optimal compliance. *International Journal of Solids and Structures 34*, 415–434.

Herencia, J. E., P. M. Weaver, and M. I. Friswell (2008). Optimization of anisotropic composite panels with T-shaped stiffeners including transverse shear effects and out-of-plane loading. *Structural and Multidisciplinary Optimization 37*(2), 165–184.

Holmberg, E., B. Torstenfelt, and A. Klarbring (2013). Stress constrained topology optimization. *Structural and Multidisciplinary Optimization 48*(1), 33–47.

Hvejsel, C. F. and E. Lund (2011). Material interpolation schemes for unified topology and multi-material optimization. *Structural and Multidisciplinary Optimization 43*(6), 811–825.

Hvejsel, C. F., E. Lund, and M. Stolpe (2011). Optimization strategies for discrete multi-material stiffness optimization. *Structural and Multidisciplinary Optimization 44*(2), 149–163.

IBM ILOG (2015). IBM ILOG CPLEX Optimization Studio V12.6.

IJsselmuiden, S. T., M. M. Abdalla, and Z. Gürdal (2008). Implementation of strength-based failure criteria in the lamination parameter design space. *AIAA Journal 46*(7), 1826–1836.

IJsselmuiden, S. T., M. M. Abdalla, O. Seresta, and Z. Gürdal (2009). Multi-step blended stacking sequence design of panel assemblies with buckling constraints. *Composites Part B: Engineering 40*(4), 329–336.

Irisarri, F.-X., A. Lasseigne, F.-H. Leroy, and R. L. Riche (2014). Optimal design of laminated composite structures with ply drops using stacking sequence tables. *Composite Structures 107*, 559–569.

Irisarri, F.-X., D. M. J. Peeters, and M. M. Abdalla (2016). Optimisation of ply drop order in variable stiffness laminates. *Composite Structures 152*, 791–799.

Johansen, L. S. and E. Lund (2009). Optimization of Laminated Composite Structures Using Delamination Criteria and Hierarchical Models. *Structural and Multidisciplinary Optimization 38*(4), 357—-375.

Johansen, L. S., E. Lund, and J. Kleist (2009). Failure Optimization of Geometrically Linear/Nonlinear Laminated Composite Structures using A Two-Step Hierarchical Model Adaptivity. *Computer Methods in Applied Mechanics and Engineering 198*, 2421–2438.

Kennedy, G. and J. Martins (2014). A parallel finite-element framework for large-scale gradient-based design optimization of high-performance structures. *Finite Elements in Analysis and Design 87*, 56–73.

Kennedy, G. J. (2016). A full-space barrier method for stress-constrained discrete material design optimization. *Structural and Multidisciplinary Optimization 54*(3), 619–639.

Kennedy, G. J. and J. R. R. A. Martins (2013). A laminate parametrization technique for discrete ply-angle problems with manufacturing constraints. *Structural and Multidisciplinary Optimization 48*(2), 379–393.

Khani, A., S. T. IJsselmuiden, M. M. Abdalla, and Z. Gürdal (2011). Design of variable stiffness panels for maximum strength using lamination parameters. *Composites Part B: Engineering 42*(3), 546–552.

Kirsch, U. (1990). ϵ-relaxed approach in topology optimization. *Structural Optimization 2*(3), 133–142.

Kiyono, C. Y., E. C. N. Silva, and J. N. Reddy (2017). A novel fiber optimization method based on normal distribution function with continuously varying fiber path. *Composite Structures 160*(Supplement C), 503–515.

Kogiso, N., L. T. Watson, Z. Gürdal, and R. T. Haftka (1994). Genetic algorithms with local improvement for composite laminate design. *Structural Optimization 7*(4), 207–218.

Kreisselmeier, G. and R. Steinhauser (1979). Systematic control design by optimizing a vector performance index. In *International federation of active controls symposium on computer-aided design of control systems, Zurich, Switzerland*, pp. 113–117.

Kristinsdottir, B. P., Z. B. Zabinsky, M. E. Tuttle, and S. Neogi (2001). Optimal design of large composite panels with varying loads. *Composite Structures 51*(1), 93–102.

Le, C., J. Norato, T. Bruns, C. Ha, and D. Tortorelli (2010). Stress-based topology optimization for continua. *Structural and Multidisciplinary Optimization 41*(4), 605–620.

Le Riche, R. and R. T. Haftka (1993). Optimization of laminate stacking sequence for buckling load maximization by generic algorithm. *AIAA Journal 31*, 951–956.

Le Riche, R. and R. T. Haftka (1995). Improved genetic algorithm for minimum thickness composite laminate design. *Composites Engineering 5*(2), 143–161.

Liu, B. and R. T. Haftka (2001, apr). Composite Wing Structural Design Optimization with Continuity Constraints. In *A01-25021*, Seattle, WA, pp. 1–12. Structural Dynamics and Materials Conference and Exhibit; American Institute of Aeronautics & Astronautics.

Liu, B., R. T. Haftka, and M. A. Akgün (2000). Two-level composite wing structural optimization using response surfaces. *Structural and Multidisciplinary Optimization 20*(2), 87–96.

Liu, D., V. V. Toropov, D. C. Barton, and O. M. Querin (2015). Weight and mechanical performance optimization of blended composite wing panels using lamination parameters. *Structural and Multidisciplinary Optimization 52*, 549–562.

Liu, D., V. V. Toropov, O. M. Querin, and D. C. Barton (2011). Bilevel Optimization of Blended Composite Wing Panels. *Journal of Aircraft 48*(1), 107–118.

Lund, E. and J. Stegmann (2005). On structural optimization of composite shell structures using a discrete constitutive parametrization. *Wind Energy 8*(1), 109–124.

Miki, M. and Y. Sugiyama (1993). Optimum design of laminated composite plates using lamination parameters. *AIAA Journal 31*, 921–922.

Mukherjee, A. and B. Varughese (2001, jan). Design guidelines for ply drop-off in laminated composite structures. *Composites Part B: Engineering 32*(2), 153–164.

Nagendra, S., D. Jestin, Z. Gürdal, R. T. Haftka, and L. T. Watson (1996). Improved genetic algorithm for the design of stiffened composite panels. *Computers & Structures 58*(3), 543–555.

Oest, J. and E. Lund (2017). Topology optimization with finite-life fatigue constraints. *Structural and Multidisciplinary Optimization*.

Overgaard, L., E. Lund, and O. Thomsen (2010). Structural collapse of a wind turbine blade. Part A: Static test and equivalent single layered models. *Composites Part A: Applied Science and Manufacturing 41*(2), 257–270.

París, J., F. Navarrina, I. Colominas, and M. Casteleiro (2009). Topology optimization of continuum structures with local and global stress constraints. *Structural and Multidisciplinary Optimization 39*(4), 419–437.

París, J., F. Navarrina, I. Colominas, and M. Casteleiro (2010). Block aggregation of stress constraints in topology optimization of structures. *Advances in Engineering Software 41*(3), 433–441.

Peeters, D. and M. Abdalla (2016). Optimization of Ply Drop Locations in Variable-Stiffness Composites. *AIAA Journal 54*(5), 1760–1768.

Rozvany, G. I. N. (1972). Grillages of maximum strength and maximum stiffness. *International Journal of Mechanical Sciences 14*(10), 651–666.

Rozvany, G. I. N. and T. Birker (1994). On singular topologies in exact layout optimization. *Structural Optimization 8*(4), 228–235.

Schmit, L. A. and B. Farshi (1973). Optimum laminate design for strength and stiffness. *Internation Journal for Numerical Methods in Engineering 7*(4), 519–536.

Seresta, O., Z. Gürdal, D. B. Adams, and L. T. Watson (2007). Optimal design of composite wing structures with blended laminates. *Composites Part B: Engineering 38*(4), 469–480.

Sigmund, O. (2007). Morphology-based black and white filters for topology optimization. *Structural and Multidisciplinary Optimization 33*(4-5), 401–424.

Sørensen, R. and E. Lund (2015). Thickness filters for gradient based multi-material and thickness optimization of laminated composite structures. *Structural and Multidisciplinary Optimization 52*(2), 227–250.

Sørensen, S. N. and E. Lund (2013). Topology and thickness optimization of laminated composites including manufacturing constraints. *Structural and Multidisciplinary Optimization 48*(2), 249–265.

Sørensen, S. N., R. Sørensen, and E. Lund (2014). DMTO - a method for Discrete Material and Thickness Optimization of laminated composite structures. *Structural and Multidisciplinary Optimization 50*(1), 25–47.

Stegmann, J. and E. Lund (2005). Discrete material optimization of general composite shell structures. *International Journal for Numerical Methods in Engineering 62*(14), 2009–2027.

Stolpe, M. and K. Svanberg (2001). An alternative interpolation scheme for minimum compliance topology optimization. *Structural and Multidisciplinary Optimization 22*(2), 116–124.

Sved, G. and Z. Ginos (1968). Structural optimization under multiple loading. *International Journal of Mechanical Sciences 10*(10), 803–805.

Tortorelli, D. and P. Michaleris (1994). Design sensitivity analysis: overview and review. *Inverse Problems in Engineering 1*, 71–105.

Tsai, S. W. and N. J. Pagano (1968). Invariant properties of composite materials. In S. W. Tsai et al (Ed.), *Composite Materials Workshop*, Volume 1 of *Progress in Material Science*, Stamfort, Connecticut, pp. 233–253. Technomic Publishing Co.

Wu, C., Y. Gao, J. Fang, E. Lund, and Q. Li (2017, aug). Discrete topology optimization of ply orientation for a carbon fiber reinforced plastic (CFRP) laminate vehicle door. *Materials & Design 128*, 9–19.

Yan, J., Z. Duan, E. Lund, and J. Wang (2017). Concurrent multi-scale design optimization of composite frames with manufacturing constraints. *Structural and Multidisciplinary Optimization*.

Yang, R. J. and C. J. Chen (1996). Stress-based topology optimization. *Structural Optimization 12*(2), 98–105.

Zein, S. and M. Bruyneel (2015). A bilevel integer programming method for blended composite structures. *Advances in Engineering Software 79*, 1–12.

Zein, S., B. Colson, and S. Grihon (2012). A primal-dual backtracking optimization method for blended composite structures. *Structural and Multidisciplinary Optimization 45*(5), 669–680.

Zein, S., V. Madhavan, D. Dumas, L. Ravier, and I. Yague (2016). From stacking sequences to ply layouts: An algorithm to design manufacturable composite structures. *Composite Structures 141*, 32–38.

Zhou, M. and R. Fleury (2012, aug). Composite Optimization - Ply Drop-Rate Constraints for Concepts and Detailed Design. In *Proceedings of the 23rd International Congress of Theoretical and Applied Mechanics (ICTAM)*. Beijing, China.

Zhou, M., R. Fleury, and M. Kemp (2011). Optimization of Composites - Recent Advances and Application. The 7th Altair CAE Technology Conference: Altair.